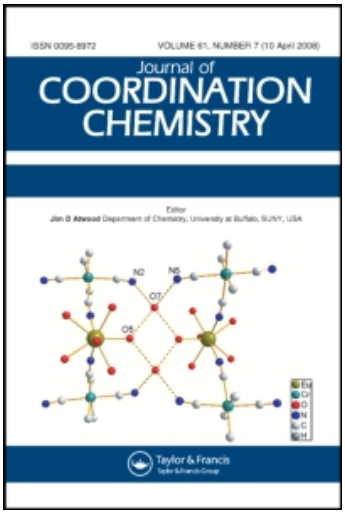

Journal of Coordination Chemistry
Publication details, including instructions for authors and subscription information:
http://www.informaworld.com/smpp/title~content=t713455674

Synthesis, characterization and antimicrobial activity of homodinuclear complexes derived from 2,6-bis[3'-methyl- 2'-carboxamidyliminomethyl(6',7')benzindole]-4-methylphenol, an end-off compartmental ligand

Y. Jadegoud[a]; Omkar B. Ijare[a]; B. S. Somashekar[a]; G. A. Nagana Gowda[a]; B. H. M. Mruthyunjayaswamy[b]
[a] Center of Biomedical Magnetic Resonance, Lucknow 226014, Uttar Pradesh, India [b] Department of Post Graduate Studies and Research in Chemistry, Gulbarga University, Gulbarga 585106, Karnataka, India

First published on: 03 September 2007

To cite this Article Jadegoud, Y. , Ijare, Omkar B. , Somashekar, B. S. , Gowda, G. A. Nagana and Mruthyunjayaswamy, B. H. M.(2008) 'Synthesis, characterization and antimicrobial activity of homodinuclear complexes derived from 2,6-bis[3'-methyl- 2'-carboxamidyliminomethyl(6',7')benzindole]-4-methylphenol, an end-off compartmental ligand', Journal of Coordination Chemistry, 61: 4, 508 — 527, First published on: 03 September 2007 (iFirst)
To link to this Article: DOI: 10.1080/00958970701362523
URL: http://dx.doi.org/10.1080/00958970701362523

Journal of Coordination Chemistry
Vol. 61, No. 4, 20 February 2008, 508–527

Taylor & Francis
Taylor & Francis Group

Synthesis, characterization and antimicrobial activity of homodinuclear complexes derived from 2,6-*bis*[3′-methyl-2′-carboxamidyliminomethyl(6′,7′)benzindole]-4-methylphenol, an end-off compartmental ligand

Y. JADEGOUD†, OMKAR B. IJARE†, B. S. SOMASHEKAR†,
G. A. NAGANA GOWDA† and B. H. M. MRUTHYUNJAYASWAMY*‡

†Center of Biomedical Magnetic Resonance, Lucknow 226014,
Uttar Pradesh, India
‡Department of Post Graduate Studies and Research in Chemistry, Gulbarga University,
Gulbarga 585106, Karnataka, India

(*Received 18 October 2006; in final form 8 March 2007*)

End-off compartmental pentadentate Schiff base, 2,6-*bis*[3′-methyl-2′-carboxamidyliminomethyl(6′,7′)benzindole]-4-methylphenol is synthesized and characterized by 2D NMR experiments and mass spectral techniques. The homodinuclear phenalato bridged end-off compartmental Schiff-base complexes Cu(II), Co(II), Ni(II), Mn(II), Fe(III), VO(IV), Zn(II), Cd(II) and Hg(II) have been prepared by the template method using the precursors 2,6-diformyl-4-methylphenol, 3-methyl(6′,7′)-2-benzindolehydrazide and metal chlorides in 1 : 2 : 2 ratio. The complexes are characterized by IR, NMR, UV-vis, FAB-mass, ESR and TGA techniques. Ni(II), Mn(II) and Fe(III) complexes have octahedral geometry, whereas the Cu(II), Co(II), VO(IV), Zn(II), Cd(II) and Hg(II) complexes have square pyramidal geometry. Low magnetic moment values for Cu(II), Co(II), Ni(II), Mn(II), Fe(III) and VO(IV) complexes indicate antiferromagnetic spin-exchange interaction between two metal centers. The metal complexes have been screened for their antibacterial activity against *Escherichia coli* and *Staphyloccocus aureus* and antifungal activity against *Aspergillus niger* and *Fusarium oxysporum*.

Keywords: End-off; Benzindole; Antiferromagnetic; Phenalato bridged

1. Introduction

Dinuclear metal cores are observed in biological systems [1]; dinuclear cores bridged by oxygen (oxo, hydroxo or water) and one or two carboxylate groups are widely known in biosites such as hemeritryne [2], ribonucleotide reductase [3] and phospholipase C [4]. Dinuclear Zn(II) cores are seen in biological systems, such as phosphatases [5] and aminopeptidases [6]. In addition, some synthetic dinuclear Zn(II) complexes have functions in RNA hydrolysis [7] and dephosphorylation [8]. The synthesis of metal complexes that can serve as structural and functional models for enzymes is of tremendous interest. In order to not only mimic the core structure found in biological

*Corresponding author. Email: bhmmswamy53@rediffmail.com

ISSN 0095-8972 print/ISSN 1029-0389 online © 2008 Taylor & Francis
DOI: 10.1080/00958970701362523

systems, but also to achieve the biological function, the development of multinucleating ligands is of great importance. Urea adducts of dinuclear nickel complexes derived from end-off ligands were studied as relevant to urease–urea interaction [9] and conversion of urea into cyanate ion (NCO^-) was achieved on dinuclear nickel(II) complexes. The μ-phenoxodi(μ-carboxylato)-dimanganese(II) [10] complexes of end-off ligands were investigated as functional models of Mn catalase and phosphatase. Vanadium chemistry has received considerable attention because of its presence in biological systems. Vanadium is an essential trace element for human beings [11] as vanadate and is known to affect phosphate metabolism. Vanadium is also an essential nutrient in higher life forms [12], where it is involved in phospolipid oxidation, sulphur metabolism and cholesterol biosynthesis [13]. There is heightened interest in the biological chemistry of vanadium due to the discovery of two types of vanadium enzymes [14], vanadium nitrogenase and vanadium bromoperoxidase. The involvement of vanadoenzymes in both reductive ($N_2 + 6H^+ + 6^{e^-} \rightarrow 2NH_3$) and oxidative ($RH + H_2O_2 + HX \rightarrow RX + 2H_2O$) transformations signifies the importance of its +3, +4 and +5 oxidation states. The synthesis and characterization of such complexes with biologically important oxidation states of vanadium help elucidate the biological role of vanadium.

Literature survey reveals that most researchers have concentrated on synthesis and characterization of various transition metal complexes using aliphatic diamines [15]. In the present study an acyclic dinucleating ligand containing the indole moiety, 2,6-*bis*[3′-methyl-2′-carboxamidyliminomethyl(6′,7′)benzindole]-4-methylphenol (**HL**) has been synthesized to develop a functional model containing a heterocyclic moiety bridged by a dinuclear metallic core. A literature [16] survey on indole derivatives gives evidence for the wide applications of indole derivatives in chemotherapy. Synthesis of new indoles is important because of their applications in various fields. To develop new functional models, we report synthesis, characterization and biological activity of 2,6-*bis*[3′-methyl-2′-carboxamidyliminomethyl(6′,7′)benzindole]-4-methylphenol (**HL**) and its Cu(II), Co(II), Ni(II), Mn(II), Fe(III), VO(IV), Zn(II), Cd(II) and Hg(II) complexes.

2. Experimental

2.1. *Material and methods*

All chemicals were of reagent grade. Solvents were dried and distilled before use according to standard procedures [17]. 2,6-Diformyl-4-methylphenol was prepared according to the method reported by Denton and Suschitzky [18]. The precursor benzindolehydrazide was prepared by literature method [19]. The metal salts used were in their hydrated form.

2.2. *Antimicrobial activity*

The *in vitro* antibacterial screening of the ligand (**HL**) and its complexes were undertaken against *Escherichia coli* and *Staphylococcus aureus* by cup-plate method using nutrient agar as medium. In a typical procedure, molten nutrient agar kept at 45°C was poured into petri dishes and allowed to solidify. Then holes of 5 mm diameter

were punched carefully using a sterile cork borer and were completely filled with test solutions (1 mg mL^{-1} in DMF). The plates were incubated for 24 h at 37°C. The diameter of the zones of inhibition for all the test compounds was measured and the results were compared with the standard drug ciprofloxacin of the same concentration as that of the test compound under identical conditions.

The antifungal activity of the test compounds was evaluated against *Aspergillus niger* and *Fusarium oxysporum* by the cup-plate method cultured on potato-dextrose agar medium adapting the procedure described above. The plates were incubated at 37°C for 48 h. The diameters of the zone of inhibition for all the test compounds were measured and the results were compared with the standard drug griseofulvin of the same concentration as that of the test compound under identical conditions.

Since all test compounds and standard drugs were prepared in freshly distilled DMF, its zone of inhibition was found to be negligible and taken as 0 mm.

2.3. *Physical measurements*

IR spectra were recorded as KBr pellets on a PERKIN-ELMER 1000 infrared spectrometer. ^{1}H NMR spectra were recorded on a Bruker Avance 400 MHz spectrometer. UV-vis spectra were recorded on an Elico SL 159 spectrophotometer in the range 200–1000 nm in DMF (1×10^{-3} M). A mass spectrum of the ligand was acquired on a MASPEC SYSTEM; the FAB mass spectra of the complexes were obtained on a JEOL SX 102/DA-6000 mass spectrometer using Argon/Xenon as the FAB gas. The accelerating voltage was 10 KV and the spectra were recorded at room temperature using meta-dinitrobenzyl alcohol as a matrix. Elemental analyses were obtained from HERAEUS C, H, N–O rapid analyzer and metal analysis was carried out by following the standard methods. ESR measurements were carried out on a VARIAN E-109 X-band spectrometer working at a microwave frequency of 9.05 GHz. The experiment was carried out by using diphenylpicrylhydrazyl (DPPH) as reference with the field set at 3200 Gauss. Magnetic susceptibilities were determined by the Faraday method using a model 300 Lewis Coil Force Magnetometer of one tesla field strength at room temperature. The instrument was calibrated with $HgCo(SCN)_4$ [20]. The degradation study of complexes has been carried out on Universal V3.2B instruments Auto TGA 2950HR V5.4A.

2.4. *Synthesis of HL*

A mixture of 2,6-diformyl-4-methylphenol (0.164 g, 0.001 mol) and 3-methyl (6′,7′)benzoindole-2-carbohydrazide (0.478 g, 0.002 mol) was refluxed in the presence of a catalytic amount of acetic acid (1–2 drops) in 30 mL methanol for 7 h on a water bath. The brown solid that separated was collected by filtration, washed with hot methanol, dried and crystallized from dioxane. Anal. Calcd for $C_{37}H_{30}N_6O_3$ (%): C, 73.26; H, 4.95; N, 13.86. Found: C, 73.24; H, 4.94; N, 13.84. Yield, 88%. M.p. 285°C. FT-IR [KBr pellet, cm^{-1}]: 2857 (hydrogen bonded-OH), 3255 (m, CONH), 3324 (m, indole NH) [21], 1674 (s, C=O), 1627 (s, C=N), 1312 (m, phenolic C–O).

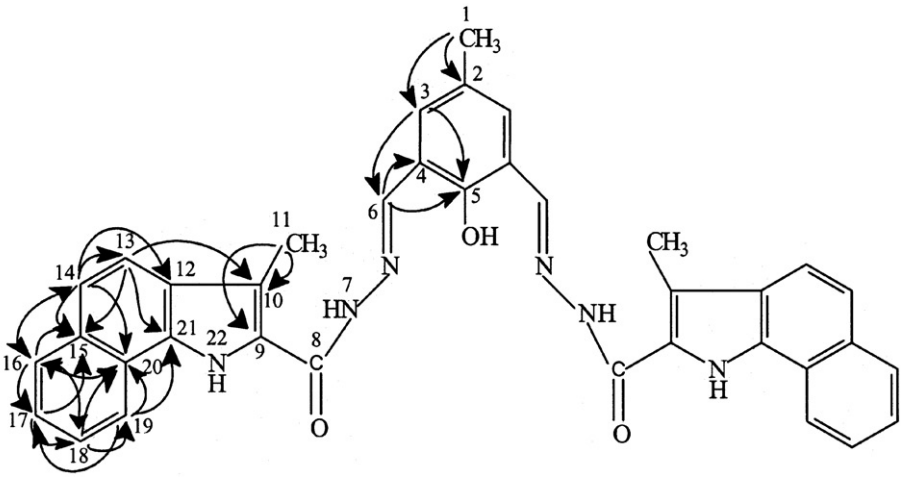

Figure 1. Structure and numbering of $^{1}H/^{13}C$ resonances of **HL**. Observed $^{1}H–^{13}C$ HMBC correlations are shown as arrow marks.

2.4.1. Two-dimensional NMR spectrum of HL. Assignment of ^{1}H chemical shifts. $^{1}H/^{13}C$ NMR (d_6-DMSO): The structure and $^{1}H/^{13}C$ numbering of the ligand **HL** is given in figure 1. The singlet at 12.18 ppm (s, H, –OH) is assigned to hydrogen bonded-OH. The H6 protons of the azomethine functions appear as a singlet at 8.68 ppm (s, 2H, 2CH=N) [11], the H7 protons of CONH appear as a singlet at 11.79 ppm (s, 2H, 2CONH). The singlet at 12.31 ppm (s, 2H, 2-indole-NH) is assigned to H22 (indole-NH). H11 protons of the two methyl groups of benzoindole moieties appear as a singlet at 2.63 ppm (s, 6H, $2CH_3$) and H1 protons of methyl group at 3-position of phenyl ring are at 2.35 ppm (s, 3H, CH_3). Chemical shifts of H3, H14, H17 and H18 protons overlap in the region 7.45–7.7 ppm. We made use of two-dimensional $^{1}H–^{1}H$ double quantum filtered correlated spectroscopy (DQF-COSY) and $^{1}H–^{13}C$ heteronuclear multiple bond correlation experiments (HMBC) to identify their ^{1}H and ^{13}C chemical shifts. Figures 2 and 3 show DQF-COSY and HMBC spectra of the ligand. The ^{1}H and ^{13}C chemical shifts are displayed in table 1. In this ligand the coupling of benzindole protons H13 and H14, H16 and H17, H18 and H19 are confirmed by COSY cross peaks.

Assignment of ^{13}C chemical shifts. Carbon resonances were grouped according to their multiplicity using SEFT (which showed positive signals for quaternary carbons and negative signals for CH and CH_3 carbons) and HSQC which shows one-bond $^{13}C–^{1}H$ correlations (figure not shown). Further, all quaternary carbons were unambiguously assigned using the spectra from quaternary carbon detection (QCD) experiments, which showed signals from quaternary carbons only [22]. Subsequently individual assignment of all the carbons was made from combinations of HSQC and HMBC spectra. Each proton in the HMBC spectra showed cross peaks to carbons that were up to three bonds away. A typical HMBC 2D spectrum of the ligand is displayed in figure 3 along with most of the assignments; HMBC correlations are depicted by arrows from

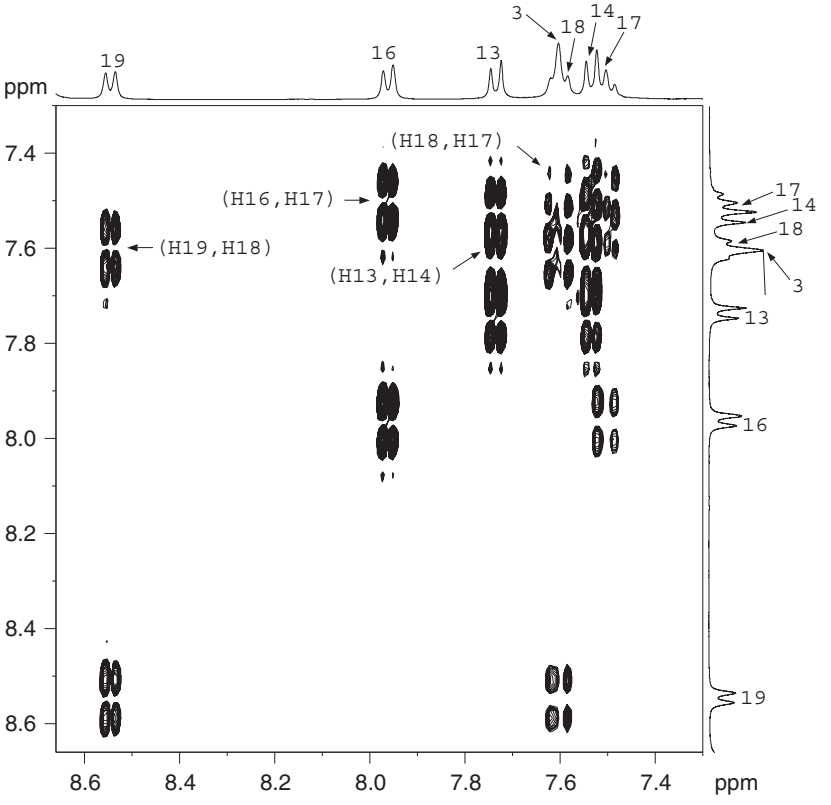

Figure 2. ^{1}H–^{1}H double-quantum filtered COSY spectrum of **HL** on a 400 MHz spectrometer, along with the assignments.

proton to carbons. Observed HMBC correlations are shown as arrows in figure 1. In the HMBC spectrum, cross peaks due to coupling of CH_3 protons to quaternary carbon C-2 and C-3 confirms the chemical shift of the CH_3 protons at the 1-position of the diformylphenyl ring. H3 protons correlation to C-2, C-4, C-5 and C-6 carbons is evident by the HMBC cross peaks. H-6 (azomethine) proton showed correlation to C-5 and C-4 carbons. The CH_3 at the 11 position of indole is confirmed by its correlation to C-9, C-10 and C-11 carbons. Peak intensities of the C-3, C-4, C-5 and C-6 carbon chemical shifts are weak, which were confirmed by the cross peaks in HMBC spectrum. The chemical shifts of amide-NH and 5-OH protons were distinguished in the ^{1}H–^{1}H total correlated spectroscopy, TOCSY (figure not shown) cross peak from correlation of indole-NH and amide-NH protons.

2.4.2. ES-MS. In the mass spectrum, the molecular ion peak corresponding to the molecular weight (606) of the ligand (**HL**) has not been observed, perhaps because the molecular ion undergoes fragmentation before reaching the detector. However, the fragment ions at m/z 426 ($M^+ - C_{13}H_{10}N^{\bullet} = A_1$, 6%), m/z 188 ($A_1 - C_{14}H_{10}N_2O^{\bullet}$, $CH_3^{\bullet}$, $H^{\bullet} = A_2$, 66%), m/z 69 ($A_2 - C_7H_4NO^{\bullet} = A_3$, 100%), m/z 369 ($A_1 - CH_3^{\bullet}$,

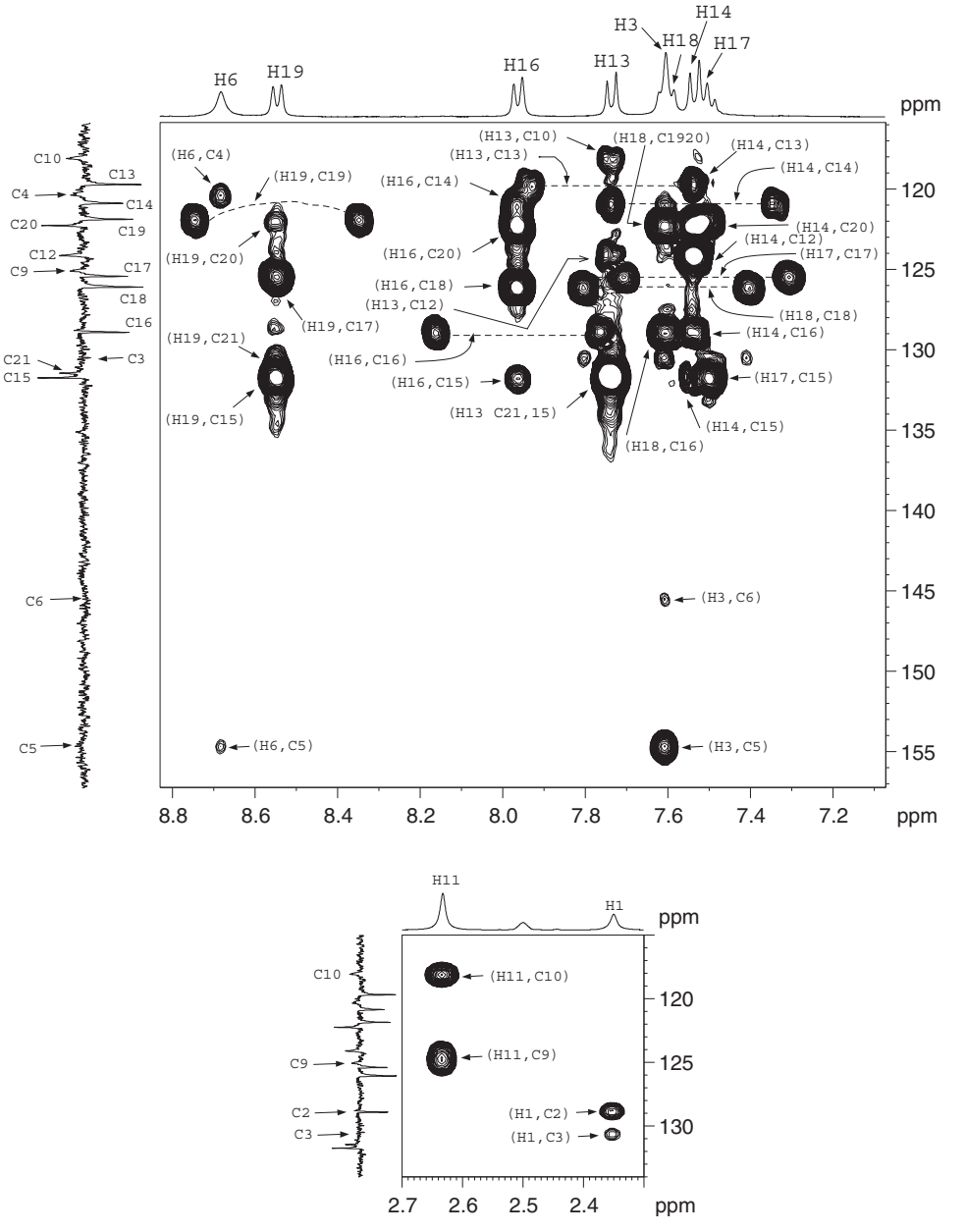

Figure 3. Typical heteronuclear multiple-bond correlation spectrum of **HL**, with the numbered assignments of cross peaks arising from one-, two-, or three-bond proton-carbon couplings. Cross peaks attributable to one-bond proton-carbon coupling for 13, 14, 16, 17, 18 and 19 are joined by horizontal dashed lines. 1-D ^{1}H and ^{13}C spectra are also projected on the top and left side of the 2-D spectrum.

$N{=}C{=}O^{\bullet} = A_4$, 4%) were observed. The mass fragmentation pattern is shown in scheme 1. Though the molecular ion in the mass spectrum of the ligand is not observed, the two-dimensional ^{1}H–^{1}H COSY and ^{1}H–^{13}C HMBC assignments unambiguously support the structure of the ligand.

Table 1. ^{1}H and ^{13}C chemical shifts of the ligand **HL**.

No.	Carbon type	^{1}H (ppm)	^{13}C (ppm)
1	CH_3	2.35	20.37
2	C	–	128.70
3	CH	7.60	130.51
4	C	–	120.88
5	C	–	154.64
6	CH	8.68	145.49
7	NH	11.79	–
8	C	–	158.84
9	C	–	125.11
10	C	–	118.11
11	CH_3	2.63	10.33
12	C	–	124.16
13	CH	7.73	119.72
14	CH	7.53	120.88
15	C	–	131.75
16	CH	7.96	128.92
17	CH	7.50	125.23
18	CH	7.60	126.10
19	CH	8.54	121.88
20	C	–	122.28
21	C	–	131.46
22	NH	12.31	–
5-OH		12.18	–

2.5. *Preparation of complexes*

Complexes of **HL** were synthesized by template method owing to its poor solubility in common organic solvents. Methanolic solution (10 mL) of 2,6-diformyl-4-methylphenol (0.164 g, 0.001 mol) was added to a benzindolehydrazide (0.478 g, 0.002 mol) in methanol (20 mL). To the resulting reaction mixture, hot solution of the metal(II) chloride (0.002 mol) in methanol (10 mL) was added and refluxed for about 6–7 h with occasional shaking on a water bath. It was then allowed to cool to room temperature, yielding the respective complexes. The solid complex was collected by filtration, washed with distilled water, then with hot methanol and dried in vacuum over anhydrous calcium chloride.

3. Results and discussion

The analytical data of the metal complexes of **HL**, table 2, suggest binuclear structures for all complexes with the empirical formula $[(VO)_2(L)(\mu\text{-}OCH_3)]\cdot 2H_2O$ for the vanadium complex and $[M_2(L)(\mu\text{-}Cl)Cl_n(H_2O)_n]\cdot nH_2O$ for the rest of the complexes. The molar conductance values (table 2) of all the complexes fall in the range for non-electrolytes indicating the non-ionic nature of the complexes.

3.1. *IR spectral studies*

The IR stretching frequencies exhibited by **HL**, as well as its complexes and their assignments are listed in table 3. In the IR spectra of all the complexes, medium

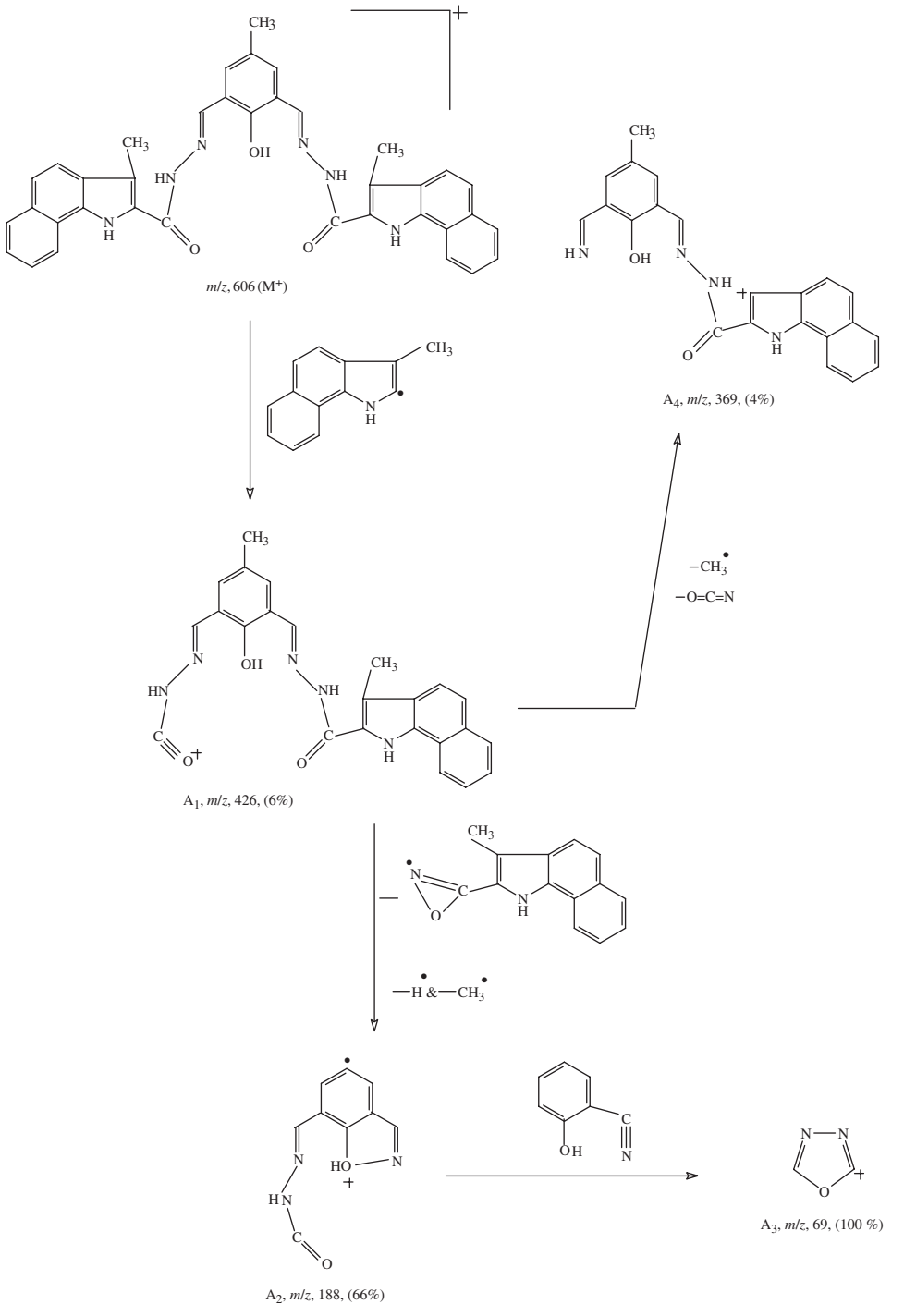

Scheme 1. Mass fragmentation patterns for the ligand HL.

Table 2. Analytical, physical and magnetic susceptibility data of complexes.

Compound empirical formula	Mol. wt	M.p./yield (°C), (%)	Analysis found (Calcd) (%)					μ_{eff} (B.M)	λ_m ($cm^2\Omega^{-1}mol^{-1}$)
			M	C	H	N	Cl		
(**HL**)$C_{37}H_{30}N_6O_3$	606	285 (88)	–	73.24 (73.26)	4.94 (4.95)	13.84 (13.86)	–	–	–
$[Cu_2(L)(\mu\text{-}Cl)Cl_2]\cdot 3H_2O$	892.5	298(d) (77)	14.21 (14.24)	49.68 (49.74)	3.90 (3.92)	9.37 (9.41)	11.95 (11.93)	1.45	51
$[Co_2(L)(\mu\text{-}Cl)Cl_2]\cdot 3H_2O$	883.3	>340 (72)	13.30 (13.34)	50.21 (50.26)	3.93 (3.96)	9.46 (9.50)	12.01 (12.05)	4.35	57
$[Ni_2(L)(\mu\text{-}Cl)Cl_2(H_2O)_2]\cdot 2H_2O$	900.8	>340 (69)	13.00 (13.02)	49.25 (49.28)	4.06 (4.10)	9.29 (9.32)	11.80 (11.82)	2.58	61
$[Mn_2(L)(\mu\text{-}Cl)Cl_2(H_2O)_2]$	857.4	>340 (69)	12.80 (12.82)	51.75 (51.78)	3.82 (3.84)	9.77 (9.79)	12.40 (12.42)	5.72	61
$[Fe_2(L)(\mu\text{-}Cl)Cl_4]\cdot H_2O$	912.1	279 (78)	12.22 (12.24)	48.64 (48.67)	3.37 (3.39)	9.18 (9.20)	19.43 (19.45)	5.76	60
$[(VO)_2(L)(\mu OCH_3)]\cdot 2H_2O$	803.8	320 (79)	12.66 (12.67)	56.70 (56.72)	4.20 (4.22)	10.42 (10.44)	–	1.28	11
$[Zn_2(L)(\mu\text{-}Cl)Cl_2]\cdot 2H_2O$	878.2	300(d) (68)	14.82 (14.89)	50.51 (50.55)	3.71 (3.75)	9.52 (9.56)	12.15 (12.12)	Diamag	55
$[Cd_2(L)(\mu\text{-}Cl)Cl_2]\cdot 2H_2O$	972.3	>300 (69)	23.10 (23.12)	45.63 (45.66)	3.35 (3.39)	8.60 (8.63)	10.92 (10.95)	Diamag.	56
$[Hg_2(L)(\mu\text{-}Cl)Cl_2]\cdot 2H_2O$	1148.	295 (68)	34.87 (34.92)	38.61 (38.65)	2.84 (2.87)	7.28 (7.31)	9.23 (9.27)	Diamag.	49

Table 3. IR spectral data of ligand and its complexes (cm^{-1}).

Compd.	ν(OH) hydrogen-bonded	$\nu(H_2O)$	ν(NH) amide/indole	ν(C=O)	ν(C=N)	ν(C–O) bridged phenolic	(C=NN=C) azine	ν(M–O)/(V=O)	ν(M–N)	ν(M–Cl)
HL ligand	2857	–	3255/3324	1674	1627	1312	–	–	–	–
Cu(II)	–	3404	3227/3333	1627	1594	1548	–	568	429	320
Co(II)	–	3432	3253/3315	1630	1586	1557	–	578	471	311
Ni(II)	–	427	3238/3325	1633	1589	1552	–	576	479	311
Mn(II)	–	3436	3252/3321	1636	1591	1552	–	575	440	308
Fe(III)	–	3421	3246/3327	1627	1578	1552	–	556	441	320
VO(IV)	–	3429	–/3344	–	1594	1539	1602	548/972	468	–
Zn(II)	–	3452	3269/3328	1639	1596	1544	–	573	475	317
Cd(II)	–	3458	3262/3318	1631	1604	1548	–	575	472	314
Hg(II)	–	3429	3235/3326	1628	1587	1562	–	565	453	318

intensity bands in the region 3269–3227 and 3344–3315 cm^{-1} are assigned to ν(CONH) (except VO(IV) complex) and ν(indole–NH) respectively, in approximately the same region as that of the ligand indicating the non coordination of amide NH and indole NH. A broad band at 2857 cm^{-1} for free ligand due to ν(hydrogen bonded-OH) was absent in all the complexes indicating involvement of phenolic oxygen in bonding with the metal ion through deprotonation. The sharp band at 1674 cm^{-1} of free ligand is attributable to ν(C=O), which is shifted to lower frequency by 35–47 cm^{-1} and appears in the range 1627–1639 cm^{-1} for all complexes except the VO(IV) complex, indicating involvement of the carbonyl in coordination. The disappearance of ν(NH) and ν(C=O) bands in the VO(IV) complex compared to the ligand proved enolisation of amide carbonyl and subsequent coordination of the enolic oxygen with the metal ions via deprotonation. Enolisation of amide was further confirmed by the appearance of a new band at 1602 cm^{-1} in the VO(IV) complex assigned to characteristic azine (C=N–N=C) formed during complexation with the metal. The absorption band at 1627 cm^{-1} for free ligand is due to ν(–C=N) [23] which shows a negative shift of 23–47 cm^{-1} and appears in the region 1580–1604 cm^{-1} for all complexes, suggesting azomethine groups coordinate to the metal ion. The medium intensity new band observed in the region 1544–1562 cm^{-1} for the dinuclear complexes are assigned to ν(M–O–M) for bridged phenolic oxygen in accordance with earlier reports [24]. In all complexes the absorption band in the region 3404–3458 cm^{-1} is due to ν(OH) of H_2O (lattice/coordinated). The new bands in the region 429–479 cm^{-1} and 548–578 cm^{-1} were assigned to ν(M–N) and ν(M–O) vibrations, respectively [25]. The oxovanadium complexes had a band at 972 cm^{-1}, assigned to ν(V=O) in accordance with earlier reports [26, 27]. The new set of bands observed in the region 308–320 cm^{-1} in all the complexes were attributed to ν(M–Cl) [28].

3.2. *Electronic spectra*

The electronic spectra of **HL** and complexes were recorded in DMF solution at 10^{-3} M. The ligand showed bands at 37,735 and 27,933 cm^{-1}. The strong absorption peaks at 37,735 cm^{-1} can be assigned to $n \rightarrow \pi^*$ transitions and a broad peak at 27,933 cm^{-1} is due to $\pi \rightarrow \pi^*$ transitions associated with azomethine [29]. In the electronic spectra of the Cu(II) complex, three bands are observed at 10,004, 14,598 and 18,050 cm^{-1} corresponding to $^2B_1 \rightarrow {}^2A_1$, $^2B_1 \rightarrow {}^2B_2$ and $^2B_1 \rightarrow {}^2E$ transitions, respectively. The observed transitions for Cu(II) are well within the range of 9000–10,000 cm^{-1}(ν_1), 11,500–16,000 cm^{-1}(ν_2) and 15,000–19,000 cm^{-1}(ν_3) reported for Cu(II) complexes of square pyramidal geometry [30, 31]. In the electronic spectrum of the Co(II) complex, three absorption bands at 11,101, 17,053 and 20,247 cm^{-1} represent the $^4A_2 + {}^4E \rightarrow {}^4B_1$, $^4A_2 + {}^4E \rightarrow {}^4E(P)$ and $^4A_2 + {}^4E \rightarrow {}^4A_2(P)$ transitions, respectively, suggesting the square pyramidal geometry for the Co(II) complex [30]. Electronic spectral data of copper and cobalt complexes suggest square pyramidal geometry for both complexes. In the Ni(II) complex bands at 10,344, 16,410 and 25,641 cm^{-1} correspond to $^3A_{2g} \rightarrow {}^3T_{2g}(\nu_1)$, $^3A_{2g} \rightarrow {}^3T_{1g}(E)(\nu_2)$ and $^3A_{2g} \rightarrow {}^3T_{1g}(P)(\nu_3)$ transitions, respectively, well within the ranges of 8000–13,000 cm^{-1}(ν_1), 15,000–19,000 cm^{-1}(ν_2) and 25,000–30,000 cm^{-1}(ν_3) reported for octahedral geometry [26, 31]. This assignment is in accord with nickel's propensity to form six-coordinated species [27]. The Mn(II) and Fe(III) complexes showed weak absorptions in the visible

region, probably due to spin-forbidden transitions [32, 33]. The Mn(II) complex exhibited four weak absorption bands at 18,018, 24,096, 28,985 and 32,258 cm^{-1}, attributed to the transitions $^6A_{1g} \rightarrow {}^4T_{1g}({}^4G)(\nu_1)$, $^6A_{1g} \rightarrow {}^4E_g({}^4G)(\nu_2)$, $^6A_{1g} \rightarrow {}^4E_g({}^4D)(\nu_3)$, and $^6A_{1g} \rightarrow {}^4T_{1g}({}^4P)(\nu_4)$, respectively. The observed transitions for Mn(II) complex in this study suggested an octahedral geometry [26]. The Fe(III) complex has three weak transitions at 16,835, 20,576, and 25,974 cm^{-1}. The d–d transitions in high spin Fe(III) complexes are generally obscured due to charge transfer absorption in the lower energy. However, the three weak bands observed in the present Fe(III) complex suggest octahedral geometry [26]. The vanadium complex has three absorption bands at 13,123, 16,420 and 22,172 cm^{-1}. The electronic spectrum of the vanadium complex is interpreted according to the Ballhausen and Gray model [34]; the difference between ν_1 and ν_2 is 3397 cm^{-1}, less than 4000 cm^{-1}, as expected for the model. Three bands are assigned to $b_2 \rightarrow e^*(^2B_2 \rightarrow {}^2E)$, $b2 \rightarrow a1^*(^2B_2 \rightarrow {}^2A_1)$ transitions and a charge transfer band, respectively. In earlier reports [35, 36] three bands in the region 12,500–13,650 cm^{-1}, 16,000–16,800 cm^{-1} and 21,000–23,500 cm^{-1} for oxovanadium complex indicate square pyramidal geometry [37].

In Zn(II), Cd(II) and Hg(II) complexes the $n \rightarrow \pi^*$ transitions are shifted to a lower wavelength 45,045, 44,444 and 45,045 cm^{-1} compared to the ligand (37,735 cm^{-1}) because the nonbonding electrons of the ligating atoms are stabilized by coordination to metal ions and the $n \rightarrow \pi^*$ energy gap increases. However, the $\pi \rightarrow \pi^*$ band at 27,933 cm^{-1} for the ligand shifts to higher wavelengths 26,041, 25,706 and 26,178 cm^{-1} for the Zn(II), Cd(II) and Hg(II) complexes, respectively. The shifts indicate that coordination of C=N groups to the metal causes the contribution of the ionic form (C^+–N^-) to increase and therefore the π bond is weakened and its energy level is shifted closer to the energy of the π^* orbital.

3.3. *^{1}H NMR of Zn(II), Cd(II) and Hg(II) complexes*

The ^{1}H NMR spectra of the complexes were recorded in DMSO-d_6. A singlet at 12.18 ppm assigned to hydrogen bonded-OH in **HL** disappears in the Zn(II) Cd(II) and Hg(II) complexes indicating involvement of OH in coordination through deprotonation. Two protons of the azomethine of the complexes are singlets at 8.70, 8.71 and 8.70 ppm (s, 2H, 2CH=N) [11], respectively, and the NH protons of CONH are singlets at 11.80, 11.80 and 11.81 ppm (s, 2H, 2CONH), respectively. In all three complexes a singlet at 12.31 ppm (s, 2H, 2-indole-NH) was assigned to indole-NH. Two methyl groups of benzoindole moieties have appeared as singlets at 2.63 ppm (s, 6H, $2CH_3$) and methyl protons at the 3-position of the phenyl ring resonate at 2.35 ppm (s, 3H, CH_3). The aromatic protons are in the region 7.59–8.54 (m, 14H, Ar–H).

3.4. *Magnetic susceptibility*

Magnetic susceptibility measurements were performed at room temperature (table 2). The magnetic moment for the Cu(II) complex is 1.45 B.M. per copper, which is less than the normal value. The lowered magnetic moment is due to antiferromagnetic spin-exchange interaction between two Cu atoms of the complex. The dinuclear Co(II) complex has a magnetic moment value of 4.35 B.M. per Co atom.

Pilkington and Robson [38] have reported lowered magnetic moment values in the range 4.3–4.6 B.M. for five-coordinate, square pyramidal Co(II) complexes. The Ni(II), Mn(II), Fe(III) and VO(IV) complexes also have lowered magnetic moments of 2.58, 5.72, 5.76 and 1.28 B.M., indicating weak antiferromagnetic coupling interactions between the metal centers [27, 37].

3.5. *ESR spectra*

The X-band ESR spectrum of the Cu(II) complex was recorded at room temperature using DPPH as a standard. The observed '*g*' values $g_{\parallel} = 2.238$ and $g_{\perp} = 2.0653$ for $[Cu_2(L)(\mu\text{-}Cl)Cl_2] \cdot 3H_2O$ complex followed the trend $g_{\parallel} > g_{\perp} > g_e$ (2.0023), suggesting an unpaired electron in the $d_{x^2-y^2}$ orbital [39] and square pyramidal geometry [40] in agreement with its electronic spectral data. The ESR spectrum of the Cu(II) complex was broad and without hyperfine splitting. In general, chloro-bridged binuclear Cu(II) complexes have a broad ESR signal [41]. The broadening of the ESR spectrum of present Cu(II) complex confirms presence of bridging chloride. The broadening was assigned to a spin-exchange interaction between two Cu-centers [42]. This antiferromagnetic spin-exchange interaction between the two metal centers is supported by the observed *g* value, which measures the spin-exchange interaction between two copper centers. *g* was found to be 3.41 [26, 43] ($g = 4$ is a characteristic feature of mononuclear complexes devoid of spin-interactions) suggesting weak antiferromagnetic spin exchange between two copper atoms.

3.6. *FAB mass spectra*

3.6.1. FAB mass spectrum of $[Cu_2(L)(\mu\text{-}Cl)Cl_2] \cdot 3H_2O$. The FAB mass spectrum of $[Cu_2(L)(\mu\text{-}Cl)Cl_2] \cdot 3H_2O$ is shown in figure 4 and its fragmentation pattern is given in scheme 2. The molecular ion (M^+) of the complex at *m*/*z* 893 is equivalent to the molecular weight of the Cu-complex. The peak at *m*/*z* 768 is the fragment ion A_1 $[Cu_2(L)(\mu\text{-}Cl)]^+$, formed by simultaneous loss of three water molecules and two chlorine radicals (–$Cl^{\bullet}$) from the molecular ion. The fragment ion A_1 with the loss of another chlorine (–$Cl^{\bullet}$) radical gave a peak at *m*/*z* 732 due to A_2 $[Cu_2(L)]^+$, which further underwent fragmentation with elimination of one benzindole moiety along with a methyl group at its 3-position and gave a peak at *m*/*z* 552 due to A_3 $[Cu_2C_{24}H_{19}N_5O_3]^+$. The fragment ion A_3 by the loss of another benzindole moiety with a methyl group at its third position yielded a peak at *m*/*z* 372, corresponding to A_4 $[Cu_2C_{11}H_9N_4O_3]^+$, which is also a base peak. The fragmentation pattern of the complex is in agreement with its structure.

3.6.2. FAB mass spectrum of $[(VO)_2(L)(\mu\text{-}OCH_3)] \cdot 2H_2O$. The FAB mass spectrum of $[(VO)_2(L)(\mu\text{-}OCH_3)] \cdot 2H_2O$ is reproduced in figure 5 and the fragmentation pattern is given in scheme 3. In the FAB mass spectrum, the molecular ion (M^+) peak observed at *m*/*z* 804 is equivalent to the molecular weight (803.88) of the complex. The molecular ion (M^+) loses two water molecules and a $-CH_3^{\bullet}$ radical giving a peak at *m*/*z* 753 due to A_1 $[(VO)_2C_{37}H_{27}N_6O_4]^+$. This fragment ion A_1 with simultaneous expulsion of two benzindole moieties and a $-CH_3^{\bullet}$ radical of

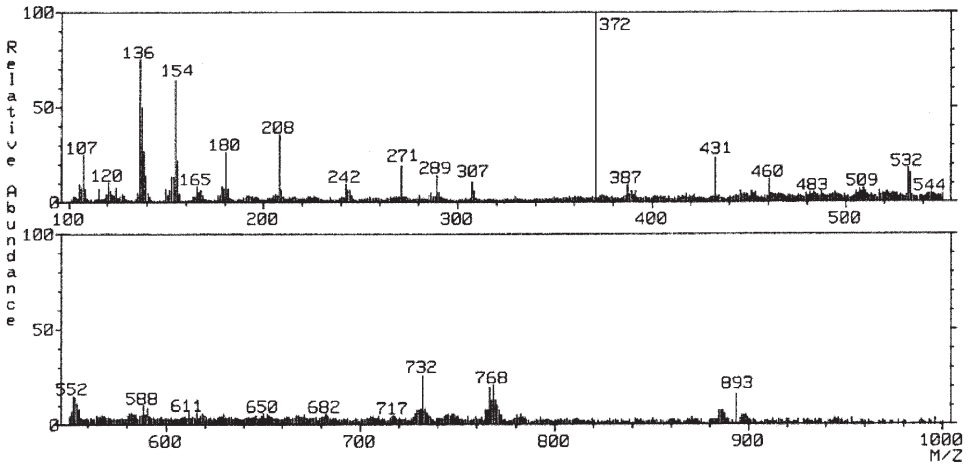

Figure 4. FAB mass spectrum of $[Cu_2(L)(\mu\text{-}Cl)Cl_2]\cdot 3H_2O$.

the 4-position of phenol, gave another ion peak at m/z 378, representing A_2 $[(VO)_2C_{10}H_4N_4O_4]^+$. The fragment ion A_1, in another way, loses one benzindole moiety giving a peak at m/z 573 due to A_3 $[(VO)_2C_{24}H_{17}N_5O_4]^+$. A_3 underwent further fragmentation with the loss of –CO and $-CH_3^{\bullet}$ radical, giving a fragment ion at m/z 530 representing A_4 $[(VO)_2C_{22}H_{14}N_5O_4]^+$, which, with loss of benzindole moiety and a $-CH_3^{\bullet}$ radical, gave a peak at m/z 350 due to A_5 $[(VO)_2C_9H_4N_4O_4]^+$. In the FAB mass spectrum the other peaks at 307, 208, 289, 154, 137, and 136 are due to *m*-nitrobenzyl alcohol used as matrix during the analysis.

3.7. *Thermogravimetric analysis*

The thermogram of $[Ni_2(L)(\mu\text{-}Cl)Cl_2(H_2O)_2]\cdot 2H_2O$, shown in figure 6, shows a first inflection point at 85–90°C with weight loss of 3.94%, accounting for loss of two lattice water molecules (3.99% calculated). Continued heating resulted in a second inflection point at 252°C with weight loss of 16.17% for loss of two coordinated water molecules and three chlorides (theoretical 16.36%). Elimination of three chlorides along with the water molecules has an exothermic peak at 250°C in the DTA curve. The third inflection point with decomposition of the dehydrated complex occurs in the temperature range 340–420°C with weight loss of 39.95%, corresponding to loss of benzindole moiety ($C_{13}H_9N$), $2CH_3$ and C_6H_5 radical (39.54% calculated). Decomposition resulted in an exothermic peak at 377°C in the DTA curve. The complex is unstable above 420°C with continuous weight loss till 700°C. The thermogravimetric analysis results are consistent with the FAB mass spectral results and the structure suggested for the complex.

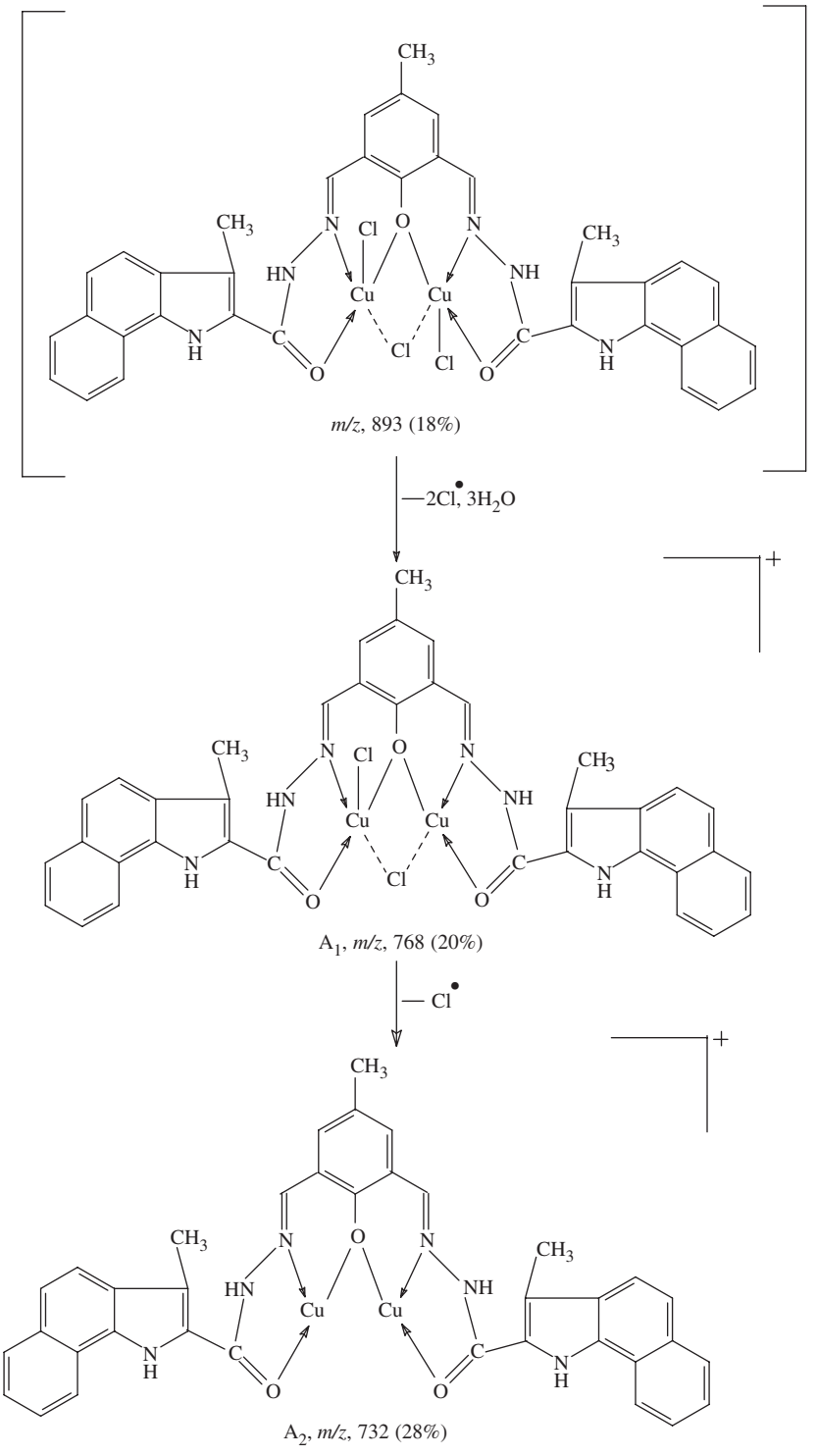

Scheme 2. FAB mass fragmentation pattern of Cu(II) complex of HL.

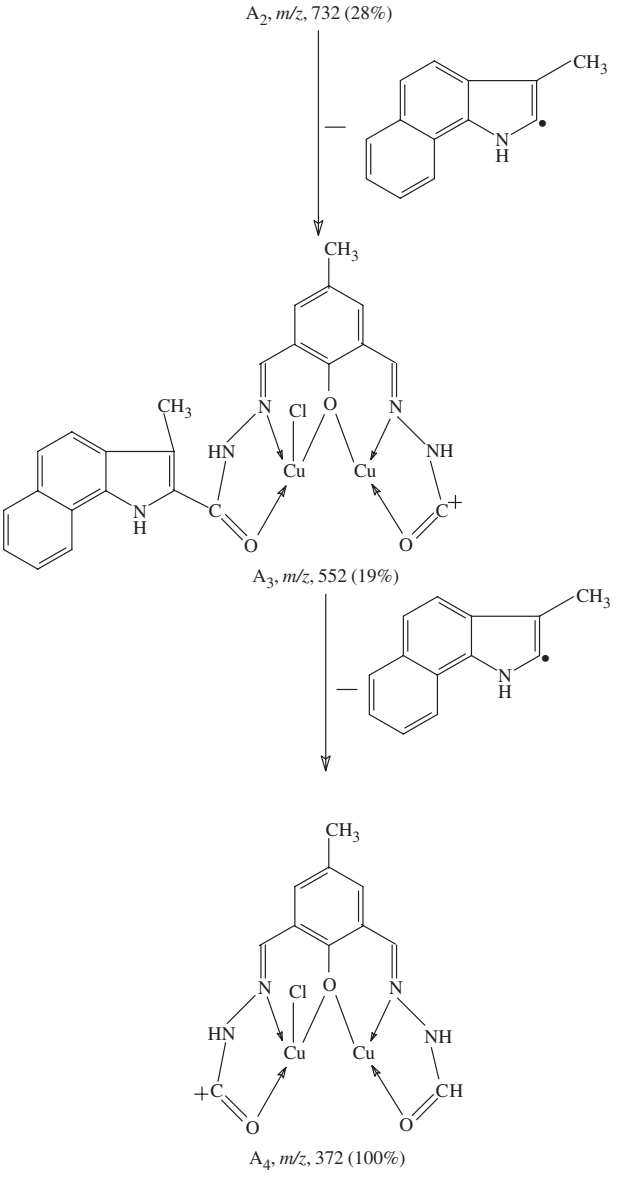

Scheme 2. Continued.

4. Antimicrobial activity

Several indole-2-carboxyhydrazides [16] have exhibited good antibacterial activity against *Micobacterium tuberculosis*. To assess the biological applications of indole derivatives in the present study, **HL** and its complexes were tested for antimicrobial activity against selected bacteria and fungi. The ligand showed antibacterial activity

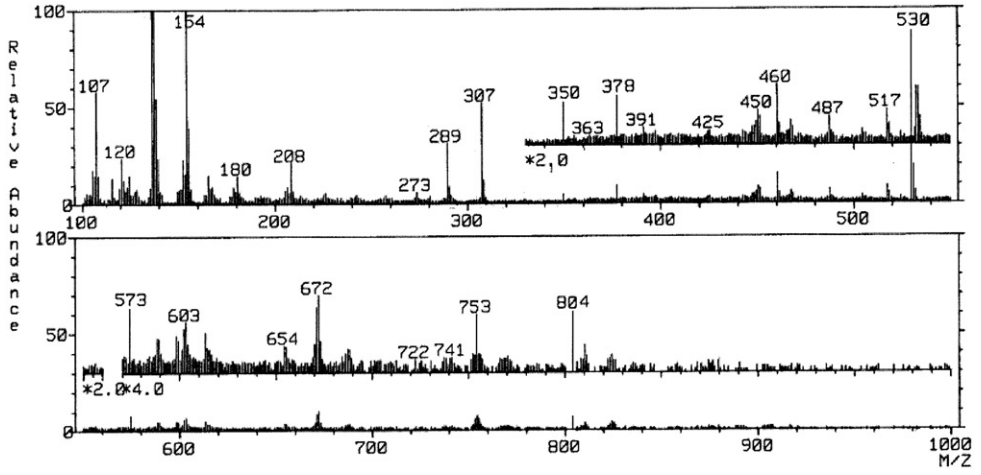

Figure 5. FAB mass spectrum of $[(VO)_2(L)(\mu\text{-}OCH_3)] \cdot 2H_2O$.

with 18 and 19 mm zones of inhibition against *E. coli* and *S. aureus* microorganisms when compared to standard drug ciprofloxacin, which showed 24 and 22 mm inhibition at $1\,mg\,mL^{-1}$ concentration against both microorganisms. The Cu(II) and Zn(II) complexes exhibited antibacterial activity with 17 & 16 mm and 18 & 17 mm inhibition against *E. coli* and *S. aureus*, respectively. The ligand **HL** exhibited antifungal activity with inhibition of 20 and 18 mm against *A. niger* and *F. oxysporum*, respectively, when compared to standard drug griseofulvin at $1\,mg\,mL^{-1}$ concentration. The Cu(II), Ni(II) and Zn(II) complexes showed antifungal activity with zones of inhibition 17, 18 & 20 mm and 16, 19 & 19 mm against *A. niger* and *F. oxysporum*, respectively. Vanadium complex showed enhanced antibacterial activity with a zone of inhibition of 21 and 20 mm and antifungal activity with a zone of inhibition of 20 and 21 mm compared to ligand.

5. Conclusion

The ligand **HL** is coordinated in pentadentate fashion to metal atoms through oxygen atoms of the two carbonyl functions and nitrogen of the azomethine groups. The dinuclear complexes are bridged by exogenous chloride, methoxy group and endogenous phenolic oxygen. The non-electrolytic behavior of the complexes confirms the presence of all chlorides within the coordination sphere. The Cu(II), Co(II), VO(IV), Zn(II), Cd(II) and Hg(II) complexes have square-pyramidal geometry, whereas Ni(II), Mn(II) and Fe(III) complexes are octahedral. The FAB mass spectral data of the Cu(II) and VO(IV) complexes are in agreement with their structures. Thermogravimetric data of the Ni(II) complex is in agreement with its structure and provide evidence for two lattice and two coordinated water molecules. The VO(IV) complex showed enhanced antimicrobial activity compared to **HL**. On the basis of

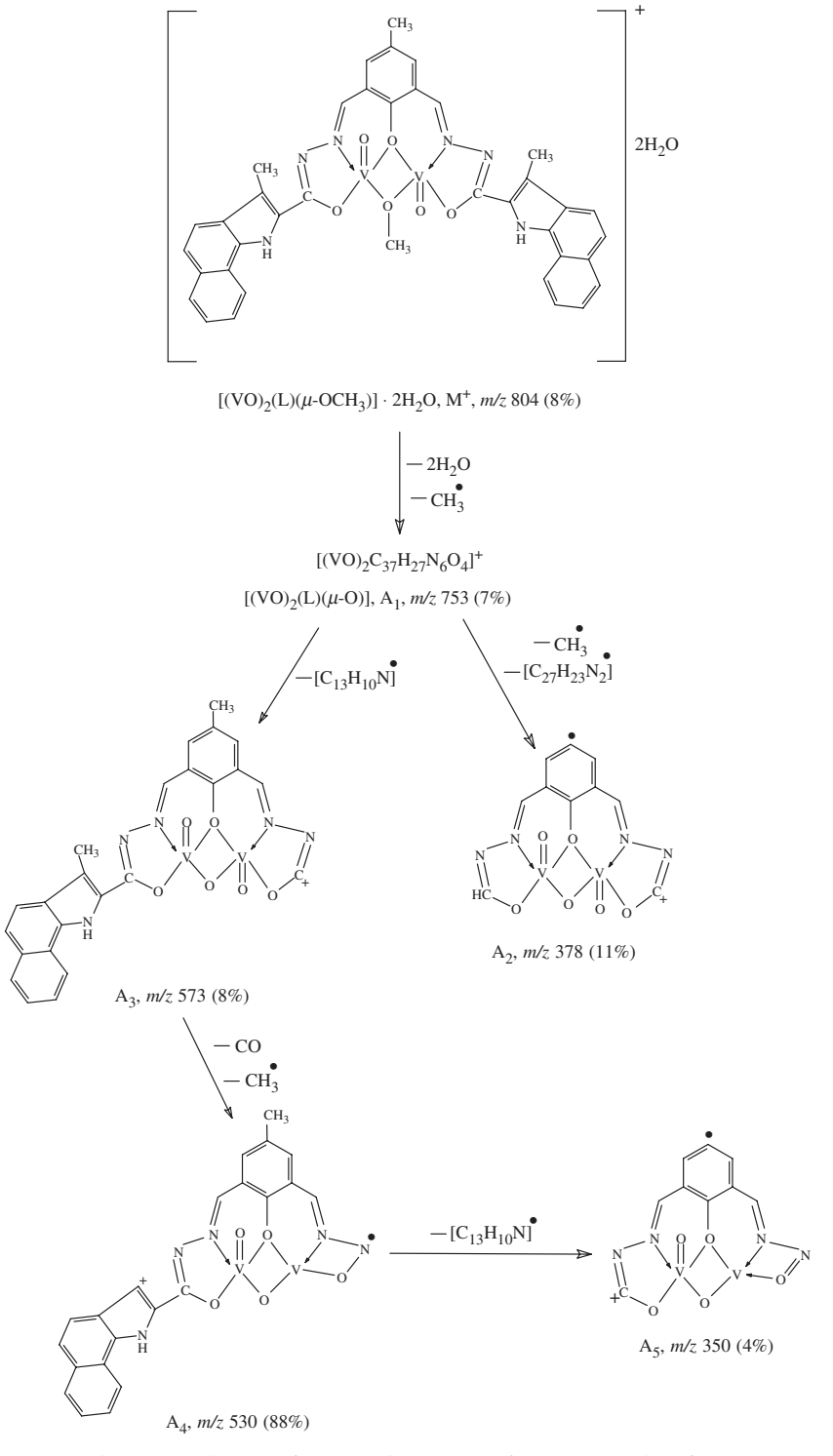

Scheme 3. FAB mass fragmentation pattern of VO(IV) complex of HL.

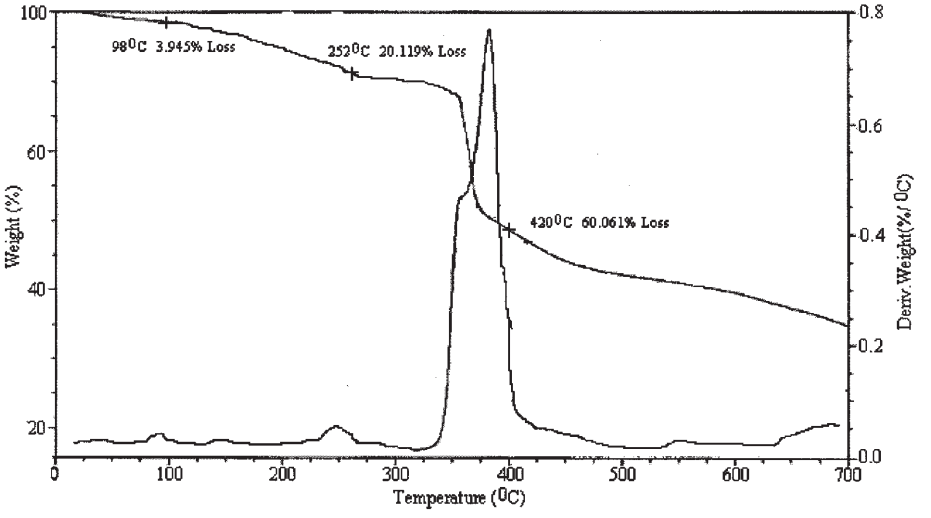

Figure 6. The thermogram of the $[Ni_2(L)(\mu\text{-}Cl)Cl_2(2H_2O)] \cdot 2H_2O$.

spectral evidences, the following structures have been assigned for the compounds.

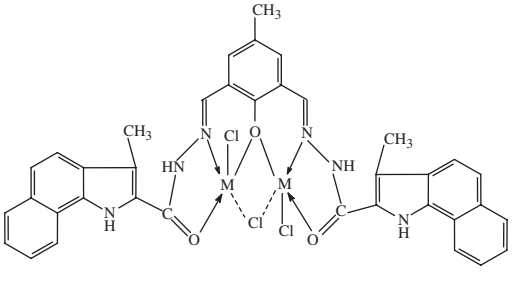

where M = Cu, Co, Zn, Cd, Hg
$Ni(H_2O)$, $Mn(H_2O)$ and $Fe(Cl)_2$

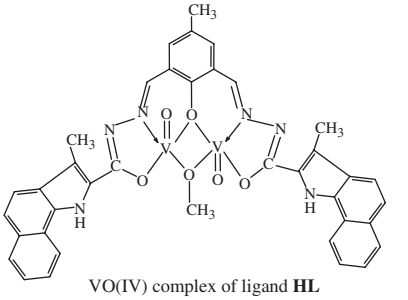

VO(IV) complex of ligand **HL**

Acknowledgments

We thank the Chairperson of the Department of Studies in Chemistry, Gulbarga University, Gulbarga, for providing research facilities. Authors are thankful to SIF, IISc Bangalore, CDRI, Lucknow, for providing ESR, Mass, and FAB mass spectral data. Authors are grateful to Prof. C.L. Khetrapal, Director, Center of Biomedical Magnetic Resonance, Lucknow, for providing NMR facility.

References

[1] D.E. Fenton, H. Okawa. *Perspectives on Bioinorganic Chemistry*, Jai Press, London (1993).
[2] M.A. Holmes, I. Le Trong, S. Turley, L.C. Sieker, R.E. Stenkamp. *J. Mol. Biol.*, **218**, 583 (1991).
[3] P. Nordlund, B.M. Sjoberg, H. Eklund. *Nature*, **345**, 593 (1990).

[4] E. Hough, L.K. Hansen, B. Brikness, K. Jynge, S. Hensen, A. Hordvik, C. Little, E.J. Dodson, Z. Derewenda. *Nature*, **338**, 357 (1989).
[5] C.G. Dealwis, L. Chen, C. Brennan, W. Mandecki, C. Abadzapatero. *Protein Eng*., **8**, 865 (1995).
[6] (a) L. Roderick, B.W. Matthews. *Biochemistry*, **32**, 3907 (1993); (b) B. Chevrier, C. Schalk, H. D'orchymont, J.M. Rondeau, D. Moras, C. Tarnus. *Structure*, **2**, 283 (1994).
[7] A. Ishikubo, M. Yashiro, M. Komiyama. *Nucleic Acids Symp. Ser*., **34**, 85 (1995).
[8] M. Suzuki, H. Kanatomi, I. Murase. *Chem. Lett*., **20**, 1745 (1981).
[9] K. Abe, J. Izume, M. Ohba, T. Yokoyama, H. Okawa. *Bull. Chem. Soc. Jpn*, **74**, 85 (2001).
[10] C. Higuchi, H. Sakiyama, H. Okawa, D.E. Fenton. *J. Chem. Soc., Dalton Trans*., 1097 (1994).
[11] E.L. Neilsen. *J. Trace Elem. Exp. Med*., **13**, 113 (2000).
[12] T.G. Hudson. *Vanadium-toxicology and Biological Significance*, Elsevier, New York (1964).
[13] G.L. Curran, R.E. Burch. *Proceedings of 1st, Annual Conference Trace Subst. Environment Health*, University of Missouri, Missouri, p. 96 (1997).
[14] L.W. Amos, D.T. Sawyer. *Inorg. Chem*., **13**, 78 (1974).
[15] (a) P.S. Zanello, P.A. Tamburini, G.A. Mazzaocchin. *Coord. Chem. Rev*., **77**, 165 (1987); (b) H. Okawa, M. Tadokoro, Y. Arateke, M. Ohaba, K. Mitsumi, M. Koidawa, M. Tomono, D.E. Fenton. *J. Chem. Soc., Dalton Trans*., 253 (1993).
[16] (a) S.P. Hiremath, S. Siddappa, M. Sirsi. *Archiv. Pharm*., **298**(6), 363 (1965); (b) S.P. Hiremath, S. Siddappa. *J. Karnataka Univ*., **6**, 1 (1964); (c) M. Kidwai, R. Venkataramanan, R. Mohan, P. Sapra. *Curr. Med. Chem*., **9**, 1209 (2002).
[17] A.I. Vogel. *Text Book of Practical Organic Chemistry*, 5th Edn, Longman ELBS Publishers, London (1989); A.I. Vogel. *Text Book of Qualitative Inorganic Analysis*, 4th Edn, Longman Group Ltd, London (1978).
[18] D.A. Denton, H. Suschitzky. *J. Chem. Soc*., 4771 (1963).
[19] S.P. Hiremath, P.S. Badami, M.G. Purohit. *Indian J. Chem*., **24B**, 1115 (1985).
[20] C.J. Connor, E.S. Sinn, E.J. Cukaskas, B.S. Deaver. *Inorg. Chim. Acta*, **32**, 29 (1979).
[21] S.P. Hiremath, B.H.M. Mruthyunjayaswamy, M.G. Purohit. *Indian J. Chem*., **16B**, 789 (1978).
[22] G.A. Nagana Gowda. *Mag. Reson. Chemistry*, **39**, 581 (2001).
[23] V.H. Revankar, V.H. Arali, V.B. Mahdle. *Indian J. Chem*., **29A**, 889 (1990).
[24] (a) J. Wang, X. Xinyou, J. Chen, Q. Lou, M. Shen, X. Huang, W. Qiangjing. *Inorg. Chim. Acta*, **256**, 121 (1997); (b) B. Srinivas, N. Arulsamy, P.S. Zacharias. *Polyhedron*, **10**(7), 731 (1991).
[25] (a) P.S. Mane, S.G. Shirodkar, B.R. Arobad, T.K. Chondherkar. *Indian J. Chem*., **40A**, 648 (2001); (b) N. Raman, A. Kulandaisamy, K. Jeyasubramanian. *Indian J. Chem*., **41A**, 942 (2002).
[26] S. Chandra, K. Gupta. *Indian J. Chem*., **40A**, 775 (2001).
[27] (a) S.M. Annigeri, A.D. Naik, U.B. Gangadharmath, V.K. Revankar, V.B. Mhale. *Trans. Metal Chem*., **27**, 316 (2002); (b) E.R. Quijano, E.D. Steven, C.L. O'Connor. *Inorg. Chim. Acta*, **177**, 29 (1980).
[28] (a) R. Malhotra, S. Kumar, Jyothi, H.R. Singal, K.S. Dhindsa. *Indian J. Chem*., **39A**, 421 (2000); (b) J.R. Ferraro. *Low Frequency Vibrations of Inorganic Coordination Compounds*, Plenum, New York (1991).
[29] R.K. Chepuri Rao, P.S. Zacharias. *Polyhedron*, **16**, 1201 (1997).
[30] D.N. Satyanarayana. *Electronic Absorption Spectroscopy and Related Techniques*, p. 246, University Press, Hyderbad (2001).
[31] A.B.P. Lever. *Inorganic Electronic Spectroscopy*, Vol. 275, Elsevier, Amsterdam (1968).
[32] A. Sreekanth, M. Joseph, H.-K. Fun, M.R. Prathapachandra Kurup. *Polyhedron*, **25**, 1408 (2006).
[33] J.E. Huheey, E.A. Keiter, R.L. Keiter. *Inorganic Chemistry*, Addison-Wesley, New York (1993).
[34] C.J. Ballhausen, H.B. Gray. *Inorg. Chem*., **25**, 111 (1962).
[35] S. Kumar, S. Pandey, O.P. Pandey, J.K. Pandey. *Indian J. Chem*., **40A**, 887 (2001).
[36] D.U. Warad, C.D. Satish, V.H. Kulkarni, S.C. Bajgur. *Indian J. Chem*., **39A**, 418 (2000).
[37] M. Sakamoto, S. Itose, T. Ishimori, N. Matsumoto, H. Okawa, S. Kida. *Bull. Chem. Soc. Jpn*, **63**, 1830 (1990).
[38] N.H. Pilkington, R. Robson. *Aust. J. Chem*., **23**, 2225 (1970).
[39] B.A. Goodman, J.B. Raynor. *Advan. Inorg. Chem. Radio Chem*., **13**, 135 (1970).
[40] M. Shakir, S.P. Varkey, I.S. Hameed. *Polyhedron*, **13**, 1335 (1994).
[41] M.C. Jain, A.K. Srivastava, P.C. Jain. *Inorg, Chem. Acta*, **23**, 199 (1977).
[42] S. Sujatha, R. Kannappan, R. Venkatesen, P. Sambasiva Rao, T.M. Rajendran. *Indian Acad. Sci. (Chem. Sci.)*, **12**, 559 (2000).
[43] (a) B.J. Hathaway, D.E. Billing. *Coord. Chem. Rev*., **6**, 143 (1970); (b) B.J. Hathaway. *Essay in Chemistry*, Academic Press, New York, **61** (1971).